

# The Limits of Quantum Information Scrambling

Ahmed A. Zahia <sup>1,\*</sup>, M. Y. Abd-Rabbou <sup>2,3,†</sup>, Atta ur Rahman <sup>2,‡</sup> and Cong-Feng Qiao <sup>2,4,§</sup>

<sup>1</sup>Department of Mathematics, Faculty of Science, Benha University, Benha, Egypt

<sup>2</sup>School of Physics, University of Chinese Academy of Science, Yuquan Road 19A, Beijing, 100049, China

<sup>3</sup>Mathematics Department, Faculty of Science, Al-Azhar University, Nasser City 11884, Cairo, Egypt

<sup>4</sup>Key Laboratory of Vacuum Physics, University of Chinese Academy of Sciences, Beijing 100049, China

(Dated: August 21, 2024)

Quantum information scrambling (QI-scrambling) is a pivotal area of inquiry within the study of quantum many-body systems. This research derives mathematical upper and lower bounds for the scrambling rate by applying the Maligranda inequality. Our results indicate that the upper bounds, lower bounds, and scrambling rates coincide precisely when local operators exhibit Hermitian and unitary operators. Crucially, the convergence or divergence of these upper and lower bounds relative to the scrambling rate is contingent upon the system's initial state. To validate our theoretical framework, we investigated the spin-star model, considering both thermal and pure initial states. Furthermore, three distinct scenarios for local operators were examined, namely single-qubit, one multi-qubit, and both multi-qubit configurations. The implantation of the ancilla or external qubit aligns the scrambling rate with the established bounds. The upper and lower bounds may diverge from the scrambling rate based on the system's initial state when both local operators are multi-qubit systems. We noticed that the scrambling rate increased as the number of qubits in local operators increased.

## I. INTRODUCTION

In the realm of non-equilibrium many-body systems, a fundamental question arises: how does quantum information encoded within the initial state propagate globally during its evolution? This query holds significant weight for physicists seeking a deeper understanding of these complex systems [1]. Parallels can be drawn between this phenomenon and the information paradox, originally postulated in the context of black holes. Research suggests that within non-classical many-body systems, information encoded in initial classical correlations remains highly entangled and dispersed throughout the system's dynamics [2–4]. Consequently, retrieving this information classically might be possible after a prolonged period, but would necessitate global measurements, a concept intrinsically linked to the notion of QI-scrambling [5].

Despite the immense importance of QI-scrambling in characterizing practical quantum systems, such as quantum computers, its precise quantification remains a significant challenge [6]. Theoretical frameworks, including conformal field theories and holographic models, have yielded valuable insights [7]. However, their applicability to real-world scenarios remains limited. To bridge this gap, researchers are actively exploring methods to quantify QI-scrambling and its connection to resourcefulness in various quantum protocols. Tools like tripartite information, which track information flow, offer valuable insights into how scrambled information propagates

[8]. Out-of-time-order correlators, which capture correlations between non-chronological measurements, provide another avenue for studying information dispersal [9, 10]. Additionally, the entanglement of operators can be used to analyze how information becomes intertwined with the system, serving as an indicator of QI-scrambling [11]. These tools, coupled with advancements in simulating complex systems, hold promise for a deeper understanding of scrambling in realistic settings. Nonetheless, future research is crucial to develop more efficient computational methods, identify universal scrambling properties, and establish links between scrambling and other quantum phenomena.

Within a quantum many-body system, let us posit that two unitary local operators  $\hat{W}_i(0)$  and  $\hat{V}_j(0)$  that commute at  $t = 0$ , i.e.,  $[\hat{W}_i(0), \hat{V}_j(0)] = 0$ , located at lattice sites  $i$  and  $j$  respectively. The impact of information scrambling on this local operator  $\hat{W}_i(0)$ , can be gleaned by examining its time evolution under the Heisenberg picture. Here, the time evolution operator  $\hat{U}(t)$  governs the system's dynamics under the influence of the many-body Hamiltonian  $\hat{H}$ . This relationship can be expressed as  $\hat{W}_i(t) = \hat{U}^\dagger(t)\hat{W}_i(0)\hat{U}(t)$ , with the unitary constraint  $i\hbar\partial_t\hat{U}(t) = \hat{H}\hat{U}(t)$  and  $[\hat{H}, \hat{W}_i(0)] \neq 0$ . One approach to quantifying information scrambling leverages the squared commutator between the local operator,  $\hat{V}_j(0)$ , and its time-evolved counterpart,  $\hat{W}_i(t)$ . This quantity is mathematically represented as [5, 12]

$$\begin{aligned} \mathcal{C}(t) &= \langle [\hat{W}_i(t), \hat{V}_j(0)]^\dagger \cdot [\hat{W}_i(t), \hat{V}_j(0)] \rangle \\ &= \langle \hat{V}_j^\dagger(0)\hat{W}_i^\dagger(t)\hat{W}_i(t)\hat{V}_j(0) \rangle - \langle \hat{W}_i^\dagger(t)\hat{V}_j^\dagger(0)\hat{W}_i(t)\hat{V}_j(0) \rangle \\ &\quad - \langle \hat{V}_j^\dagger(0)\hat{W}_i^\dagger(t)\hat{V}_j(0)\hat{W}_i(t) \rangle + \langle \hat{W}_i^\dagger(t)\hat{V}_j^\dagger(0)\hat{V}_j(0)\hat{W}_i(t) \rangle, \end{aligned} \quad (1)$$

here  $\langle \dots \rangle = \text{Tr}[\hat{\rho} \dots]$  is expectation value, which  $\hat{\rho}$  can

\* ahmed.zahia@fsc.bu.edu.eg

† m.elmalky@azhar.edu.eg

‡ attazaib5711@gmail.com

§ qiaocf@ucas.ac.cn

be taken in the thermal average at inverse temperature  $\beta$  with  $\hat{\rho} = e^{-\beta\hat{H}}/\text{Tr}[e^{-\beta\hat{H}}]$ , or the initial pure state  $\hat{\rho} = |\psi\rangle\langle\psi|$ . In the context of a nonintegrable Hamiltonian, persistent  $[\hat{W}_i(t), \hat{V}_j(0)] \neq 0$ , manifested as a non-vanishing quantity  $\mathcal{C}(t)$ , i.e.  $\mathcal{C}(t) > 0$ , engenders a significant and sustained decrease in the negative parts of the equation  $\mathcal{C}(t)$  [12]. Conversely, within the framework of a non-scrambling Hamiltonian, the negative parts of  $\mathcal{C}(t)$  exhibit a revival, approaching a value close to unity, accompanied by a near-commuting relationship between  $\hat{W}(t)$  and  $\hat{V}_j(0)$ , i.e.  $[\hat{W}_i(t), \hat{V}_j(0)] \cong 0$  [13].

The motivation underpinning this paper is multifaceted. Primarily, we seek to redefine the relationship between QI-scrambling and its boundaries within the Maligranda inequality. This study aims to determine the extent to which these limits converge and to identify the potential factors contributing to any discrepancies in their behaviour. We examine the nature of QI-scrambling within a spin-star model, considering local operators both unitary-Hermitian single-spin operators or arbitrary multi-spin operators. Further, the feasibility of controlling the scrambling within the system is discussed, through two different initial states. The paper is organized as: In Sec. II, we introduce the upper and lower bounds of QI-scrambling rate by applying the Maligranda inequality, while the considered Hamiltonian structure as well as the results are given in Sec. III. We summarize the study in Sec. IV.

## II. SCRAMBLING AND UNCERTAINTY PRINCIPLE:

If  $x$  and  $y$  are nonzero vectors in a normed linear space, the Maligranda inequality is given by [14]

$$\left\| \frac{x}{\|x\|} - \frac{y}{\|y\|} \right\| \leq \frac{\|x - y\| + \left| \|x\| - \|y\| \right|}{\max\{\|x\|, \|y\|\}}, \quad (2)$$

Likewise, the other inequality,

$$\left\| \frac{x}{\|x\|} - \frac{y}{\|y\|} \right\| \geq \frac{\|x - y\| - \left| \|x\| - \|y\| \right|}{\min\{\|x\|, \|y\|\}}, \quad (3)$$

Next, let us denote  $|x\rangle = \bar{A}|\bar{x}\rangle$  and  $|y\rangle = \bar{B}|\bar{y}\rangle$ , where  $\bar{A} = \hat{A} - \langle\hat{A}\rangle$  and  $\bar{B} = \hat{B} - \langle\hat{B}\rangle$ , with  $\hat{A}, \hat{B}$  are any arbitrary operators. Then, we have

$$\|x\| = \Delta\hat{A}, \quad \|y\| = \Delta\hat{B}, \quad \text{and, } \|x - y\| = \Delta(\hat{A} - \hat{B}) \quad (4)$$

where,  $\Delta^2\hat{O} = \langle\hat{O}^2\rangle - \langle\hat{O}\rangle^2$  is the variance of operator  $\hat{O}$ . Also, we can get

$$\left\| \frac{x}{\|x\|} - \frac{y}{\|y\|} \right\| = \left[ 2 - \frac{2 \text{Re}(\text{Cov}(\hat{A}, \hat{B}))}{\Delta\hat{A}\Delta\hat{B}} \right]^{1/2}. \quad (5)$$

Here,  $\text{Cov}(\hat{A}, \hat{B}) = \langle\hat{A}^\dagger\hat{B}\rangle - \langle\hat{A}^\dagger\rangle\langle\hat{B}\rangle$  is the covariance.

From Eqs. (2) to (5) we get

$$2 - \mathcal{J}^2 \geq \frac{2\text{Re}[\text{Cov}(\hat{A}, \hat{B})]}{\Delta\hat{A}\Delta\hat{B}} \geq 2 - \mathcal{K}^2, \quad (6)$$

where

$$\mathcal{J} = \frac{\Delta(\hat{A} - \hat{B}) - |\Delta\hat{A} - \Delta\hat{B}|}{\min[\Delta\hat{A}, \Delta\hat{B}]}, \quad (7)$$

$$\mathcal{K} = \frac{\Delta(\hat{A} - \hat{B}) + |\Delta\hat{A} - \Delta\hat{B}|}{\max[\Delta\hat{A}, \Delta\hat{B}]}.$$

If we choice  $\hat{A} = \hat{V}_j(0)\hat{W}_i(t)$  and  $\hat{B} = \hat{W}_i(t)\hat{V}_j(0)$ , with Eq. (1), we get

$$\mathcal{C}(t) = \langle\hat{A}^\dagger\hat{A}\rangle + \langle\hat{B}^\dagger\hat{B}\rangle - \langle\hat{A}^\dagger\hat{B}\rangle - \langle\hat{B}^\dagger\hat{A}\rangle. \quad (8)$$

Using Eqs. (6), and (8), the QI-scrambling bounds are

$$\mathcal{L}(t) \leq \mathcal{C}(t) \leq \mathcal{U}(t), \quad (9)$$

where

$$\mathcal{L}(t) = \Delta\hat{A}\Delta\hat{B}(\alpha^2 - 2) + \|\hat{A}\|_2^2 + \|\hat{B}\|_2^2 - 2\text{Re}[\langle\hat{B}^\dagger\rangle\langle\hat{A}\rangle],$$

$$\mathcal{U}(t) = \Delta\hat{A}\Delta\hat{B}(\beta^2 - 2) + \|\hat{A}\|_2^2 + \|\hat{B}\|_2^2 - 2\text{Re}[\langle\hat{B}^\dagger\rangle\langle\hat{A}\rangle], \quad (10)$$

where  $\|\hat{O}\|_2^2 = \text{Tr}[\hat{\rho}\hat{O}^\dagger\hat{O}]$  is the square of the Hilbert-Schmidt norm of  $\hat{O}$ .

If we choice the operators  $\hat{W}(t), \hat{V}(0)$  are unitary and Hermitian, then

$$\Delta\hat{A} = \sqrt{1 - \langle\hat{W}_i(t)\hat{V}_j(0)\rangle\langle\hat{V}_j(0)\hat{W}_i(t)\rangle}, \quad (11)$$

$$\Delta\hat{B} = \sqrt{1 - \langle\hat{V}_j(0)\hat{W}_i(t)\rangle\langle\hat{W}_i(t)\hat{V}_j(0)\rangle}.$$

Thus

$$\mathcal{J} = \mathcal{K} = \frac{\Delta(\hat{A} - \hat{B})}{\Delta\hat{A}}. \quad (12)$$

So, the upper and lower bounds coincide with QI-scrambling, then

$$\mathcal{L}(t) = \mathcal{U}(t) = \mathcal{C}(t) = 2(1 - \text{Re}[\langle\hat{A}^\dagger\hat{B}\rangle]). \quad (13)$$

For only Hermitian operator, the equivalence of the three bounds is contingent upon the system's initial state.

## III. STRUCTURE OF THE HAMILTONIAN SYSTEM

Consider a quantum system comprising a two-level ancilla interacting with an ensemble of  $N$  identical spin-1/2 structure to form a spin-star model. These spins exhibit mutual interactions, see FIG. 1. The coupling between the central ancilla and the peripheral spins is assumed

to be isotropic, characterized by a coupling strength denoted as  $J_1$ . This interaction paradigm is commonly referred to as the  $XXX$ -configuration. Simultaneously, the peripheral spins interact with its neighbours, with a coupling strength  $J_2$ . The physical Hamiltonian governing this system can be expressed as (with  $\hbar = 1$ )

$$\hat{H} = \hat{H}_{free} + \hat{H}_{an-sp} + \hat{H}_{sp-sp}. \quad (14)$$

Here, the free Hamiltonian  $\hat{H}_{free} = \omega_a \hat{S}_z^a + \omega_s \sum_{i=1}^N \hat{S}_z^i$ , where  $\omega_a$  and  $\omega_s$  represent the frequencies of the ancilla and the outer spin system, respectively. The operators  $\hat{S}_z^a$  and  $\hat{S}_z^i$  correspond to the  $z$ -Pauli spin-1/2 matrices for the ancilla and  $i^{th}$  outer spins. The interaction Hamiltonian between the ancilla and the outer spins is represented by  $\hat{H}_{an-sp} = J_1 \sum_{i=1}^N (\hat{S}_x^a \hat{S}_x^i + \hat{S}_y^a \hat{S}_y^i + \hat{S}_z^a \hat{S}_z^i)$ , with  $J_1$  coupling strength. Additionally, the spin-spin interaction Hamiltonian is expressed as  $\hat{H}_{sp-sp} = J_2 \sum_{i=1}^N \vec{S}^i \cdot \vec{S}^{i+1}$ , with the coupling  $J_2$  and periodic boundary condition is imposed, such that  $\vec{S}^{N+1} = \vec{S}^1$ .

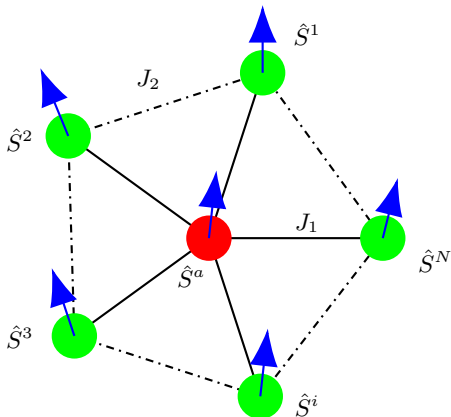


FIG. 1. A schematic representation of a central spin  $\hat{S}^a$  (red) surrounded by a collection of peripheral spins  $\hat{S}^i$  (green). The central spin interacts with each peripheral spin via a coupling constant  $J_1$ , while the peripheral spins interact with each other via a coupling constant  $J_2$ .

Our analysis is predicated on some contrasting scenarios. In the first, the two local operators are chosen from the ancilla operators or we posit that the ancilla remains in a stationary state while at least one outer spin undergoes temporal evolution, as represented by

$$\hat{V}_a(0) = \{\hat{S}_z^a, \hat{S}_x^a\} \quad \text{and} \quad \hat{W}_i(0) = \{\hat{S}_z^i, \hat{S}_x^i\}^{i=\{a,1\}}. \quad (15)$$

Conversely, in the second scenario, the central ancilla maintains a constant state while at least four outer spins experiences temporal evolution, expressed as

$$\begin{aligned} \hat{W}_i(0) &= \left\{ \sum_{i=1}^m \hat{S}_z^i, \sum_{i=1}^m \hat{S}_x^i \right\}, \quad \text{and} \\ \hat{V}_a(0) &= \{\hat{S}_z^a, \hat{S}_x^a\}. \end{aligned} \quad (16)$$

However, the third scenario the local operators are consists of some spins from the outer spins as

$$\begin{aligned} \hat{W}_i(0) &= \left\{ \sum_{i=1}^m \hat{S}_z^i, \sum_{i=1}^m \hat{S}_x^i \right\}, \quad \text{and} \\ \hat{V}_i(0) &= \left\{ \sum_{i=m+1}^N \hat{S}_z^i, \sum_{i=m+1}^N \hat{S}_x^i \right\}. \end{aligned} \quad (17)$$

In this discussion, we will scrutinize the degree of concordance between the upper bounds  $\mathcal{U}(t)$ , the lower bounds  $\mathcal{L}(t)$ , and the QI-scrambling  $\mathcal{C}(t)$ . We postulate that the internal ancilla qubit is in resonance with the external spin ensemble. Within this system, the external spin count is quantified as five ( $N = 5$ ), with spins coupled to the ancilla via a coupling constant  $J_1 = 1$  and to their counterparts through a coupling constant  $J_2 = 0.5$ . This analysis will encompass both thermal state or pure state. For thermal state  $\langle e^{\beta \hat{H}} \dots \rangle / \langle e^{\beta \hat{H}} \rangle$ , we have  $\beta = 1$ . For the initial pure state, we assume the ancilla in excited and the outer spins in the ground states, with  $|\psi\rangle = |\uparrow\rangle_a \otimes |\downarrow\rangle^{\otimes 5}$ . To further examine the influence of these variables, the supplementary data, incorporating QuTip Python code encapsulating the test outcomes [15], will be addressed. When visualizing the results, a circular representation will be employed within each graphical depiction to signify the selection of local operators  $\hat{W}_i(0)$  and  $\hat{V}_j(0)$  from the system and the corresponding qubit count. A chromatic distinction will be implemented, with red, green, and black circles denoting qubits associated with  $\hat{W}_i(0)$ ,  $\hat{V}_j(0)$ , and those excluded from selection, respectively

### A. The maximum value of scrambling for unitary-Hermitian operators

For this proposal, the QI-scrambling using unitary-Hermitian operators  $\hat{W}_i(0), \hat{V}_j(0)$  is given by

$$\begin{aligned} \mathcal{C}(t) &= \left\| [\hat{W}_i(t), \hat{V}_j(0)] \right\|_2^2 = \left\| \hat{W}_i(t) \hat{V}_j(0) - \hat{V}_j(0) \hat{W}_i(t) \right\|_2^2 \\ &\leq \left( \left\| \hat{W}_i(t) \hat{V}_j(0) \right\|_2 + \left\| \hat{V}_j(0) \hat{W}_i(t) \right\|_2 \right)^2 \\ &= 4. \end{aligned} \quad (18)$$

From this analysis, it is evident that the scrambling phenomenon is not invariably reliant on the dimensions of local operators, a notion often emphasized in some papers. However, in the present case, regardless of the dimensions of local operators, the maximum value of QI-scrambling is less than or equal to four, as long as these operators maintain their Hermitian-unitary characteristics.

FIG. 2 presents the behavioral analysis of functions  $\mathcal{L}(t)$ ,  $\mathcal{U}(t)$ , and  $\mathcal{C}(t)$  under diverse configurations of local operators  $\hat{W}_i(0)$  and  $\hat{V}_j(0)$ , constrained by the unitary and Hermitian properties. A striking observation is

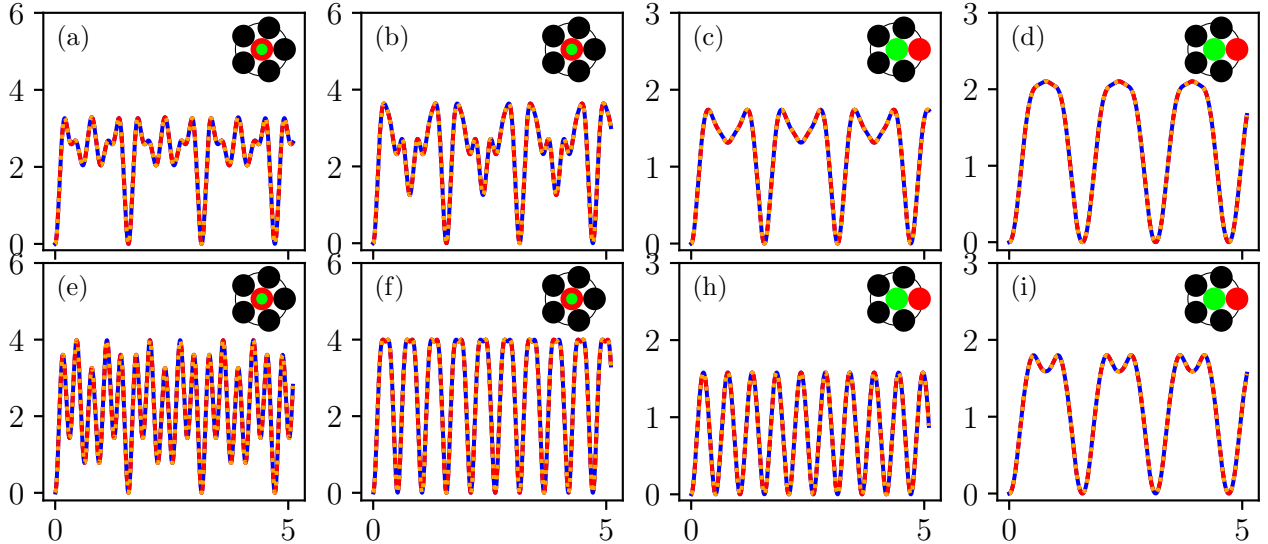


FIG. 2. The general behaviour of lower bounds  $\mathcal{L}(t)$  (orange-curve), QI-scrambling  $\mathcal{C}(t)$  (red curve) and upper bounds  $\mathcal{U}(t)$  (blue curve), where  $N = 5$ , and  $J_1 = 1$ ,  $J_2 = 0.5$ . The upper panels for thermal state with  $\beta = 1$ , (a)  $\hat{W}_a(0) = \hat{V}_a(0) = \hat{S}_x^a$ . (b)  $\hat{W}_a(0) = \hat{V}_a(0) = \hat{S}_z^a$  (c)  $\hat{W}_i(0) = \hat{S}_z^{i=1}$ ,  $\hat{V}_a(0) = \hat{S}_z^a$ . (d)  $\hat{W}_i(0) = \hat{S}_x^{i=1}$ ,  $\hat{V}_a(0) = \hat{S}_z^a$ . The lower panels for the initial pure state  $|\psi\rangle = |\uparrow\rangle_a \otimes |\downarrow\rangle^{\otimes 5}$ , (e,f,g,h) the same as  $\hat{W}_i(0)$  and  $\hat{V}_a(0)$  in (a,b,c,d).

the perfect congruence between upper and lower bounds, in tandem with scrambling, irrespective of the system's thermal or pure state. Instances where  $\hat{W}_a(0) = \hat{V}_a(0) = \hat{S}_x^a$  (FIG. 2 (a), and (e)) or  $\hat{W}_a(0) = \hat{V}_a(0) = \hat{S}_z^a$  (FIG. 2 (b), and (f)) exhibit periodic fluctuations of all three functions between a maximal value of  $\mathcal{C}(t) = [0, 4]$  within the pure state domain. Conversely, in the thermal regime, these functions asymptotically approach the maximal value while maintaining oscillatory patterns. Notably, the selection of one local operator from the ancilla coupled with another from a solitary outer spin qubit, regardless of alignment ( $\hat{W}_i(0) = \hat{S}_z^{i=1}$ ,  $\hat{V}_a(0) = \hat{S}_z^a$  FIG. 2 (c), and (h)) or orthogonality ( $\hat{W}_i(0) = \hat{S}_x^{i=1}$ ,  $\hat{V}_a(0) = \hat{S}_z^a$ , FIG. 2 (d), and (i)), results in an approximate halving of the maximal values for all three functions. A general principle emerges, the scrambling effect remains bounded by a maximum value of  $\mathcal{C}(t) \leq 4$  within the single unitary and Hermitian operators.

### B. The maximum scrambling for multi-partite local operators

Let the operators  $\hat{W}_i(0)$  and  $\hat{V}_j(0)$  consist of  $m$  and  $n$  number of multi-partite system. Such that

$$\begin{aligned} \hat{W}_i(0) &= \hat{w}_1(0) + \hat{w}_2(0) + \dots + \hat{w}_m(0) = \sum_{l=1}^m \hat{w}_l(0), \\ \hat{V}_j(0) &= \hat{v}_1(0) + \hat{v}_2(0) + \dots + \hat{v}_n(0) = \sum_{k=1}^n \hat{v}_k(0). \end{aligned} \quad (19)$$

Here,  $\hat{w}_l(0)$ , and  $\hat{v}_k(0)$  are arbitrary multi-partite operators.

Then

$$\begin{aligned} \mathcal{C}(t) &= \left\| [\hat{W}_i(t), \hat{V}_j(0)] \right\|_2^2 = \left\| \left[ \sum_l^m \hat{w}_l(t), \sum_k^n \hat{v}_k(0) \right] \right\|_2^2 \\ &\leq \sum_l^m \sum_k^n \left\| [\hat{w}_l(t), \hat{v}_k(0)] \right\|_2^2 = n^2 m^2 \mathcal{M}, \end{aligned} \quad (20)$$

where  $\mathcal{M} = \max[C_{lk}(t)]$  is the maximum scrambling  $\forall l, k$ .

We now consider the scenario wherein the influencer  $\hat{W}_i(0)$  comprises  $m$  outer spins, while  $\hat{V}_j(0)$  is associated with the ancilla. A discernible disparity emerges between the upper bounds, scrambling, and lower bounds as evidenced in FIG. 3, manifest in both thermal and pure states. This discrepancy is contingent upon the selection of the initial state for the local influencers. When,  $\hat{W}_i(0) = \sum_{i=1}^4 \hat{S}_x^i$  and  $\hat{V}_a(0) = \hat{S}_x^a$ , inequality given in Eq. (9) holds, with the disparity attributed to the difference between  $\alpha$  and  $\beta$  in Eq. (10), stemming from the differential between  $\mathcal{J}$  and  $\mathcal{K}$ . In the instance of  $\hat{W}_i(0) = \sum_{i=1}^4 \hat{S}_z^i$  and  $\hat{V}_a(0) = \hat{S}_z^a$ , a divergence is observed between the upper and lower bound values, accompanied by scrambling in the thermal state, whereas complete convergence of the three bounds is evident in the pure state where  $\mathcal{J} = \mathcal{K}$ . Notwithstanding the apparent behavioral similarity among  $\mathcal{U}(t)$ ,  $\mathcal{C}(t)$ , and  $\mathcal{L}(t)$  in the thermal regime, they exhibit non-identical characteristics. The chasm between the three bounds widens in the pure state due to the pronounced disparity between

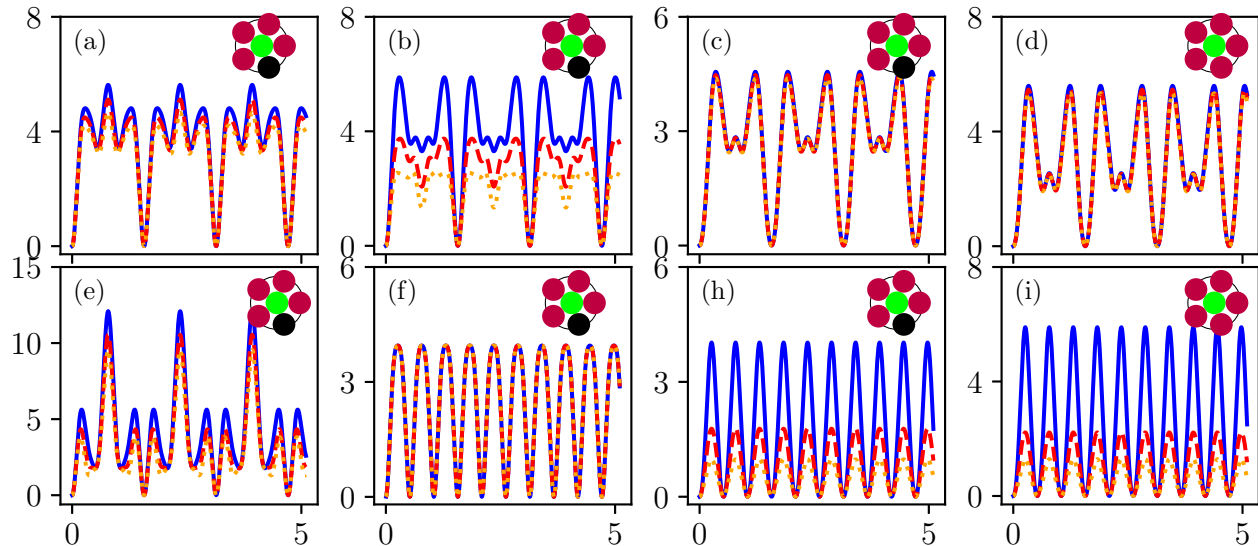


FIG. 3. The general behaviour of lower bounds  $\mathcal{L}(t)$  (orange-curve), QI-scrambling  $\mathcal{C}(t)$  (red curve) and upper bounds  $\mathcal{U}(t)$  (blue curve), where  $N = 5$ , and  $J_1 = 1$ ,  $J_2 = 0.5$ . The upper panels for thermal state with  $\beta = 1$ , (a)  $\hat{W}_i(0) = \sum_{i=1}^4 \hat{S}_x^i$ ,  $\hat{V}_a(0) = \hat{S}_x^a$ . (b)  $\hat{W}_i(0) = \sum_{i=1}^4 \hat{S}_z^i$ ,  $\hat{V}_a(0) = \hat{S}_z^a$ . (c)  $\hat{W}_i(0) = \sum_{i=1}^4 \hat{S}_x^i$ ,  $\hat{V}_a(0) = \hat{S}_x^a$ . (d)  $\hat{W}_i(0) = \sum_{i=1}^5 \hat{S}_x^i$ ,  $\hat{V}_a(0) = \hat{S}_x^a$ . The lower panels for the initial pure state  $|\psi\rangle = |\uparrow\rangle_a \otimes |\downarrow\rangle^{\otimes 5}$ , (e,f,g,h) the same as  $\hat{W}_i(0)$  and  $\hat{V}_a(0)$  in (a,b,c,d).

$\Delta\hat{A}$  and  $\Delta\hat{B}$ , exacerbated by an increase in the number of outer spins which concomitantly elevates the maximal values of all three functions. It is noteworthy that despite the substantial divergence between  $\mathcal{U}(t)$ ,  $\mathcal{C}(t)$ , and  $\mathcal{L}(t)$  remains confined within the maximum scrambling range established by Eq. (20). It is incontrovertible that altering the initial state yields disparate outcomes, yet all states are circumscribed by the identical maximal scrambling range.

Within the context of examining scrambling on the outer spins, while excluding the ancilla from the local operators, FIG. 3 reveals a random and irregular scrambling behavior across all studied scenarios. A marked convergence is observed among the upper bounds, scrambling, and lower bounds within the thermal state, with complete overlap of all three metrics, when  $\hat{W}_i(0) = \sum_{i=1}^2 \hat{S}_x^i$  and  $\hat{V}_j(0) = \sum_{j=3}^5 \hat{S}_x^j$ . Significantly, scrambling is most pronounced in this condition compared to other investigated states. Conversely, the pure state exhibits a pronounced divergence between the three bounds, although maintaining a consistent qualitative trend, suggesting that the functions  $\mathcal{U}(t)$  and  $\mathcal{L}(t)$  effectively quantify scrambling. Furthermore, a general pattern emerges where an increase in the number of qubits within  $\hat{W}_i(0)$  correlates with an expanding disparity between the three bounds and a corresponding reduction in the maximal scrambling value.

### C. Experimental and Future Prospects

QI-scrambling has emerged as a crucial area of study in quantum physics, with far-reaching implications [16].

The phenomenon of scrambling describes the rapid and complex evolution of quantum states, where the initial information becomes extensively dispersed and obscured, rendering it inaccessible to local observations [5]. This process is of paramount importance in understanding the dynamics of complex quantum systems, such as black holes [17], many-body systems [13, 18], and quantum information [19, 20]. Experimental investigations of QI-scrambling have yielded valuable insights, demonstrating the exponential growth of quantum information spreading, a hallmark of scrambling dynamics, using platforms like trapped ions [21], superconducting circuits [22], and Rydberg atom arrays [23]. These experiments have provided empirical evidence for the existence of quantum chaos, where small perturbations can lead to drastic changes in the system's behavior, akin to the butterfly effect observed in classical chaotic systems. Moreover, a universal framework to understand how QI-scrambles in open systems is introduced [24]. This framework of QI-scrambling could also be useful for interpreting signals from Loschmidt echo experiments, which have been challenging to explain. The effects of additional factors such as noise and errors on scrambling in open systems are not well understood. Exact numerical simulations for a spin system coupled to an environment is provided [25].

The examination of spin-star configurations considered in our case holds great promise for developments in quantum technologies [26]. Investigating the dynamics and associated correlations within these quantum many-body systems provide deeper understanding and insights into the behavioral aspects of such systems, allowing us to develop advanced quantum simulators and the realization of realistic quantum computing [27]. Additionally,

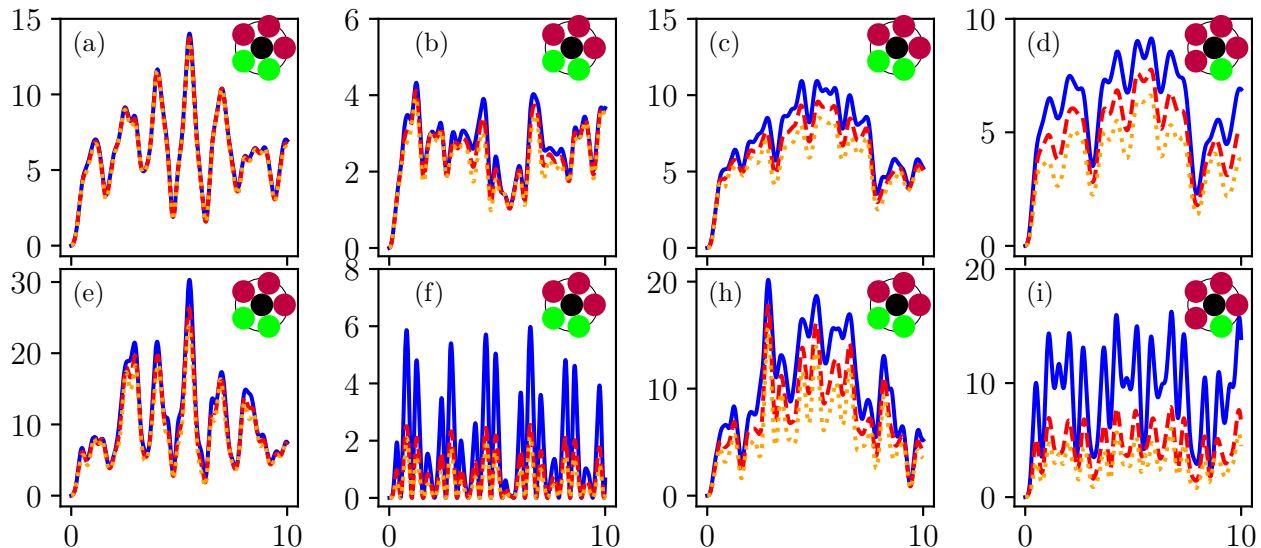


FIG. 4. The general behaviour of lower bounds  $\mathcal{L}(t)$  (orange curve), QI-scrambling  $\mathcal{C}(t)$  (red curve) and upper bounds  $\mathcal{U}(t)$  (blue curve), where  $N = 5$ , and  $J_1 = 1$ ,  $J_2 = 0.5$ . The upper panels for thermal state with  $\beta = 1$ , (a)  $\hat{W}_i(0) = \sum_{i=1}^2 \hat{S}_x^i$ ,  $\hat{V}_j(0) = \sum_{j=3}^5 \hat{S}_x^j$ , (b)  $\hat{W}_i(0) = \sum_{i=1}^2 \hat{S}_z^i$ ,  $\hat{V}_j(0) = \sum_{j=3}^5 \hat{S}_z^j$ , (c)  $\hat{W}_i(0) = \sum_{i=1}^2 \hat{S}_x^i$ ,  $\hat{V}_j(0) = \sum_{j=3}^5 \hat{S}_x^j$ , (d)  $\hat{W}_i(0) = \sum_{i=1}^4 \hat{S}_z^i$ ,  $\hat{V}_j(0) = \hat{S}_x^5$ . The lower panels for the initial pure state  $|\psi\rangle = |\uparrow\rangle_a \otimes |\downarrow\rangle_b^{\otimes 5}$ , (e,f,g,h) the same as  $\hat{W}_i(0)$  and  $\hat{V}_j(0)$  in (a,b,c,d).

the spin-star complex system exhibit unique properties which may lead to improvements in quantum sensing and metrology, therefore, enhancing the detection and measurement with high precision [28]. Furthermore, examination of the quantum phase transitions and critical phenomena in the considered spin-star models could bring new quantum phases and emergent behavioral aspects in quantum communication and information protocols [29].

The significance of the results entails that the dependence of the scrambling bounds on the local operator selection highlights the necessity to pay attention to the choice of the operator to properly describe the quantum information scrambling. The fact that Hermitian-unitary operators give the same scrambling bounds and non-unitary operators give the upper limit of scrambling for a system, gives useful insights into how to design quantum systems and protocols such that they operate in the optimized scrambling regime. Most importantly, we found that the increase in the number of qubits increases scrambling, implying that complex quantum systems are more irreversible. Additionally, the fact that the scrambling bounds and stochastically due to the initial state can merge creates more opportunities to have better quantum state preparation and stabilization with prospects in quantum information processing in computation, communication, sensing, and simulation. By understanding how local operator selection, scrambling behaviour, and multi-partite interactions affect a quantum system, researchers can better design quantum systems that are either robust against errors or deliberately scrambled to secure information.

#### IV. CONCLUSION

This study has established a mathematical relationship linking QI-scrambling to the upper and lower bounds defined by Maligranda's inequality. Our analyses indicate that scrambling is uniformly constrained by or equivalent to the Maligranda bound. Additionally, the maximum value of two arbitrary local Hermitian-unitary operators has been proven. The robustness of these correlations has been demonstrated through diverse scenarios within the spin-star model, considering both thermal and pure initial states.

Results highlight the critical influence of local operator selection on the alignment between the derived bounds and scrambling behavior. When the chosen local operator comprises Hermitian-unitary operators, perfect consistency is observed. Conversely, non-unitary local operators yield a valid correlation but lack consistency, representing the system's upper scrambling limit. Furthermore, the impact of multi-qubit systems on QI-scrambling has been rigorously investigated. The analysis reveals that the introduction of multiple qubits enhances scrambling, signifying the system's irreversible departure from its initial state over time. Intriguingly, the initial state gives rise to a convergence of the three scrambling bounds and stochastic behaviour, even in the presence of multi-qubit local operators.

## ACKNOWLEDGEMENT

This work was supported in part by National Natural Science Foundation of China(NSFC) under the Grants 11975236 and 12235008, and University of Chinese Academy of Sciences.

- 
- [1] R. Lewis-Swan, A. Safavi-Naini, A. Kaufman, and A. Rey, Dynamics of quantum information, *Nature Rev. Phys.* **1**, 627 (2019).
- [2] A. Bhattacharyya, L. K. Joshi, and B. Sundar, Quantum information scrambling: from holography to quantum simulators, *Eur. Phys. J. C* **82**, 458 (2022).
- [3] S. H. Shenker and D. Stanford, Black holes and the butterfly effect, *J. High Energy Phys* **2014**, 1 (2014).
- [4] Y. Sekino and L. Susskind, Fast scramblers, *J. High Energy Phys.* **2008** (10), 065.
- [5] B. Swingle, G. Bentsen, M. Schleier-Smith, and P. Hayden, Measuring the scrambling of quantum information, *Phys. Rev. A* **94**, 040302 (2016).
- [6] B. Fauseweh, Quantum many-body simulations on digital quantum computers: State-of-the-art and future challenges, *Nature Commun.* **15**, 2123 (2024).
- [7] C. T. Asplund, A. Bernamonti, F. Galli, and T. Hartman, Entanglement scrambling in 2d conformal field theory, *J. High Energy Phys.* **2015** (9), 1.
- [8] O. Schnaack, N. Bölter, S. Paeckel, S. R. Manmana, S. Kehrein, and M. Schmitt, Tripartite information, scrambling, and the role of hilbert space partitioning in quantum lattice models, *Phys. Rev. B* **100**, 224302 (2019).
- [9] S. Gopalakrishnan, D. A. Huse, V. Khemani, and R. Vasseur, Hydrodynamics of operator spreading and quasiparticle diffusion in interacting integrable systems, *Phys. Rev. B* **98**, 220303 (2018).
- [10] V. Khemani, D. A. Huse, and A. Nahum, Velocity-dependent lyapunov exponents in many-body quantum, semiclassical, and classical chaos, *Phys. Rev. B* **98**, 144304 (2018).
- [11] J. Harris, B. Yan, and N. A. Sinityn, Benchmarking information scrambling, *Phys. Rev. Lett.* **129**, 050602 (2022).
- [12] J. R. González Alonso, N. Yunger Halpern, and J. Dressel, Out-of-time-ordered-correlator quasiprobabilities robustly witness scrambling, *Phys. Rev. Lett.* **122**, 040404 (2019).
- [13] D. Yuan, S.-Y. Zhang, Y. Wang, L.-M. Duan, and D.-L. Deng, Quantum information scrambling in quantum many-body scarred systems, *Phys. Rev. Res.* **4**, 023095 (2022).
- [14] L. Maligranda, Simple norm inequalities, *Am. Math. Mon.* **113**, 256 (2006).
- [15] J. R. Johansson, P. D. Nation, and F. Nori, Qutip: An open-source Python framework for the dynamics of open quantum systems, *Comp. Phys. Comm.* **183**, 1760 (2012).
- [16] K. A. Landsman, C. Figgatt, T. Schuster, N. M. Linke, B. Yoshida, N. Y. Yao, and C. Monroe, Verified quantum information scrambling, *Nature* **567**, 61 (2019).
- [17] P. Hayden and J. Preskill, Black holes as mirrors: quantum information in random subsystems, *J High Energy Phys.* **2007**, 120 (2007).
- [18] E. Iyoda and T. Sagawa, Scrambling of quantum information in quantum many-body systems, *Phys. Rev. A* **97**, 042330 (2018).
- [19] N. Yunger Halpern, A. Bartolotta, and J. Pollack, Entropic uncertainty relations for quantum information scrambling, *Commun. Phys.* **2**, 92 (2019).
- [20] K. K. Sharma and V. P. Gerdt, Quantum information scrambling and entanglement in bipartite quantum states, *Quantum Inf. Process.* **20**, 195 (2021).
- [21] M. K. Joshi, A. Elben, B. Vermersch, T. Brydges, C. Maier, P. Zoller, R. Blatt, and C. F. Roos, Quantum information scrambling in a trapped-ion quantum simulator with tunable range interactions, *Phys. Rev. Lett.* **124**, 240505 (2020).
- [22] X. Mi, P. Roushan, C. Quintana, S. Mandra, J. Marshall, C. Neill, F. Arute, K. Arya, J. Atalaya, R. Babush, *et al.*, Information scrambling in quantum circuits, *Science* **374**, 1479 (2021).
- [23] T. Hashizume, G. S. Bentsen, S. Weber, and A. J. Daley, Deterministic fast scrambling with neutral atom arrays, *Phys. Rev. Lett.* **126**, 200603 (2021).
- [24] T. Schuster and N. Y. Yao, Operator growth in open quantum systems, *Phys. Rev. Lett.* **131**, 160402 (2023).
- [25] M. Knap, Entanglement production and information scrambling in a noisy spin system, *Phys. Rev. B* **98**, 184416 (2018).
- [26] J. Joshi and T. S. Mahesh, Experimental investigation of a quantum battery using star-topology NMR spin systems, *Phys. Rev. A* **106**, 042601 (2022).
- [27] P. Estarellas, *Spin chain systems for quantum computing and quantum information applications*, Ph.D. thesis, University of York (2018).
- [28] L. Gassab, O. Pusuluk, and Ö. E. Müstecaphoğlu, Geometrical optimization of spin clusters for the preservation of quantum coherence, *Phys. Rev. A* **109**, 012424 (2024).
- [29] D. Jakab and Z. Zimborás, Quantum phases of collective SU (3) spin systems with bipartite symmetry, *Phys. Rev. B* **103**, 214448 (2021).